Surface & Coatings Technology 393 (2020) 125746

Contents lists available at ScienceDirect

Surface & Coatings Technology

journal homepage: www.elsevier.com/locate/surfcoat

Titanium-supported W-containing PEO layers enriched with Mn or Zn in oxidative desulfurization and the zwitterionic liquid effect

A.A. Bryzhin[a], I.G. Tarkhanova[a], M.G. Gantman[b], V.S. Rudnev[c], M.S. Vasilyeva[c,d], I.V. Lukiyanchuk[c,*]

[a] M.V. Lomonosov Moscow State University, Moscow, Russia
[b] Friedrich-Alexander Universität Erlangen-Nürnberg, FAU, Erlangen, Germany
[c] Institute of Chemistry, Far Eastern Branch, Russian Academy of Sciences, Vladivostok, Russia
[d] Far Eastern Federal University, Vladivostok, Russia

ARTICLE INFO

Keywords:
Plasma electrolytic oxidation
$MnWO_4$- and $ZnWO_4$-containing coatings
Titanium-supported catalysts
Oxidative desulfurization
Zwitterionic liquid effect
Surface behavior

ABSTRACT

Titanium-supported oxide layers of W, W + Zn and W + Mn, formed by plasma electrolytic oxidation, were established to catalyze the peroxide oxidation of thiophene. The most active compositions based on Zn-W-containing PEO layers were also tested in the oxidation of a number of organosulfur compounds and diesel fuel desulfurization. Preliminary covering the samples by zwitterionic liquid (ZIL) made it possible to achieve residual sulfur content as low as 6 ppm. The change in the morphology and composition of samples with and without ZIL was studied during catalytic tests. It was found that ZIL reduces the etching of the sample surfaces when interacting with the reaction medium.

1. Introduction

The directed formation of active compositions on the surface of a solid support to simultaneously achieve both high catalytic activity and chemical and thermal stability is the most important problem of heterogeneous catalysis. Oxide coatings that meet these requirements can be formed on the surface of valve metals in electrolytes of suitable composition under electric spark and microarc discharges, that is, by plasma electrolytic oxidation (PEO) technique [1,2]. Regulation of PEO synthesis conditions can contribute to the creation of highly efficient catalytic systems. Metal-supported catalysts formed with using the PEO technique are studied in the reactions of deep oxidation of CO [3] and hydrocarbons [4], afterburning of exhaust gases [5], oxidation of hydrogen [6], oxidative dehydrogenation of cyclohexane [7], dehydration of alcohols [8], steam reforming of naphthalene [9], photocatalytic decomposition of organic pollutants [10], and electrochemical evolution of oxygen [11].

In accordance with applicable environmental standards, various approaches to producing fuels with ultra-low sulfur content (< 10 ppm) are considered [12]. The traditional hydrotreatment process is ineffective with respect to heterocyclic compounds [13], for example, dibenzothiophene. Therefore, an important task is the search for alternative methods of processing hydrocarbon raw materials.

Due to its high efficiency and mild conditions, oxidative desulfurization is a promising hydrogen free technology aimed at increasing the polarity of sulfur-containing substances followed by their removal by adsorption or extraction [14]. The mechanism and conditions of this process directly depend on the choice of oxidizing agent and catalyst. Oxygen [15], ozone [16], nitrogen dioxide [17], organic peroxides [18], hydrogen peroxide [19] are usually used as an oxidizing agent, and compositions containing individual and mixed oxides or salts of transition metals in high oxidation states can serve as catalysts [20–22].

Previously we found aluminum- or titanium-supported PEO layers based on oxygen compounds of W [23], Ce, and Zr [24] to be potential candidates as catalysts in oxidative desulfurization. Later studies showed that mixed oxide layers containing W and other transition metals, in particular Zn, are most effective [25]. The positive effect of Zn additives to polytungstates on catalysis is associated with the formation of mixed oxometallates, whose active center has increased electrophilicity, which is necessary for peroxidation of a sulfur-containing substrate [26]. The promoting effect of Mn additives to tungsten oxide layers was described in [23]. However, we did not investigate further on the evolution and the stability of such mixed oxide layers during the oxidation reaction. Meanwhile, for testing the catalysts, we use the model process of thiophene oxidation (the most difficultly oxidized compound among thiophene derivatives) with hydrogen

* Corresponding author.
E-mail address: lukiyanchuk@ich.dvo.ru (I.V. Lukiyanchuk).

https://doi.org/10.1016/j.surfcoat.2020.125746
Received 27 February 2020; Received in revised form 2 April 2020; Accepted 5 April 2020
Available online 07 April 2020

peroxide, which leads to the formation of sulfuric acid. Under such conditions, 'PEO layer/valve metal' catalysts can lose activity due to corrosion. Using Ce, Zr-containing catalysts as an example, we found that their pretreatment with a zwitterionic compound, such as - 4-(3′-ethylimidazolium)-butanesulfonate, prevents corrosion [24]. Furthermore, this treatment helps to increase the activity of the compositions. The concept of using ionic liquid (IL) or ZIL to stabilize the active phase of heterogeneous catalysts and increase their efficiency is called a solid catalyst with ionic liquid layer (SCILL) [27,28].

Another important factor that allows increasing the efficiency of catalysis by slowing down the side process of hydrogen peroxide decomposition is the fractional loading of the oxidizing agent. We used this approach, well known in the literature [29,30], in studies on the thiophene oxidation of on catalysts of various nature [24,31].

In the present work, we used the entire set of the above-described approaches to increase the activity and stability of W-, Mn- and W-, Zn-containing PEO-coated catalysts in the oxidation of typical sulfur-containing compounds of oil: thiophene, dibenzothiophene (DBT) and methyl phenyl sulfide. For comparison, samples containing only tungsten(VI) oxides were studied.

Thus, the aim of the work is to perform a comparative analysis of the composition and structure of titanium-supported W, W−Zn, and W−Mn PEO layers as well as their catalytic properties in the thiophene oxidation. The most active composition will be studied during peroxidation of sulfur-containing compounds and the effect of the ZIL treatment on its surface structure, activity and stability will be established. Based on the testing of the selected sample in the desulfurization of diesel fuel, we will be able to answer the question of whether our proposed approaches will allow us to obtain raw materials that meet modern environmental requirements for sulfur content (< 10 ppm).

2. Experimental

2.1. Plasma electrolytic formation of titanium-supported composites

Oxide layers were formed on VT1–0 titanium (99.9% Ti) samples of a size of 20 × 20 × 0.5 mm. As a pretreatment the samples were chemically polished in a mixture of concentrated acids ($HF:HNO_3$ = 1:3, volume relation) at 70 °C in order to remove the surface layer of natural oxide film and standardize the surface. Then the samples were washed with running and distilled water, and air-dried at room temperature.

Electrolytes were prepared using commercially available chemicals: $Na_2WO_4{\cdot}2H_2O$, NaOH, $Mn(CH_3COO)_2{\cdot}4H_2O$, and $Zn(CH_3COO)_2{\cdot}2H_2O$ of analytical grade, glacial CH_3COOH of reagent grade, 0.05 M H_2SO_4 (standard titrimetric substance) and distilled water. The compositions of the electrolytes used and the designations of the catalysts obtained in them are indicated in Table 1. Acetic acid or sulfuric acid was introduced to avoid alkalization of the electrolyte during PEO and to reduce the degree of hydrolysis of metal cations. As it was established earlier in [32], the pH of electrolyte containing only sodium tungstate increases by 3–4 units during PEO treatment due to the formation of WO_3 in the coating composition. In addition, acetate buffer (base electrolyte 2 in Table 1) was used to stabilize the pH.

PEO treatment of titanium samples was carried out at a constant effective current density of 0.2 A/cm^2 for 10 min. The electrochemical cell consisted of a thermal glass of 1 L in volume with a spiral-shaped hollow nickel cathode. The electrolyte was agitated by a magnetic stirrer. The system was cooled by cold water pumped through the cathode to keep the electrolyte temperature below 25 °C. TP4-500/460N-2 thyristor unit (Russia) operating in a unipolar mode was used as a current source. After PEO treatment, the samples were rinsed by distilled water and dried in air at room temperature.

2.2. Composites characterization

The X-ray diffraction (XRD) patterns of the coated samples were recorded on a D8 Advance X-ray diffractometer using the Bragg-Bretano method with rotation of the sample in CuK_α-radiation. The corresponding analysis was carried out using the EVA retrieval program based on the PDF-2 database.

To determine the elemental composition of the coatings and examine their surface microstructure, a Hitachi S-5500 scanning electron microscope (SEM) (Japan) equipped with a Thermo Scientific accessory for energy dispersive X-ray spectroscopy (EDS) analysis was used. The depth of scanning beam penetration was about 1 μm. Gold was preliminarily sputtered on the sample surfaces for preventing surface charging. Using EDS, we investigated both the average elemental composition of surface areas of 60 × 80 μm and the composition of characteristic formations, focusing the analyzing beam on smaller areas (from 50 × 50 nm and larger). The compositions of the surface areas were found as average of at least 5 measurements.

Note that prior to microscopic investigation, the PEO-coated samples with the deposited ZIL (before and after catalytic tests) were dried in nitrogen atmosphere at 150 °C for 4 h. This operation was performed to avoid contaminating the analyzer with volatile organic substances.

The thickness of PEO coatings was measured using an eddy-current thickness gage VT-201 (Russia) and was calculated as the average of at least 10 separate thickness measurements on both sides of a flat sample.

2.3. Catalytic tests and deposition of zwitterionic liquid

Before catalytic tests, PEO-coated samples of size 20 × 20 × 0.5 mm were cut into 8 approximately equal parts with a surface area of ~1 cm^2 and a weight of ~0.1 g.

The H_2O_2 oxidation of model substrates (thiophene, thioanizole, dibenzothiophene) was conducted in the following way: a 1 wt% mixture of a sulfur-containing compounds in isooctane (10 mL) and the catalyst (0.1 g) were placed into a thermostated reactor, the solution was heated to 60 °C, and 50% H_2O_2 (0.4 mL) was added. The fractional loading was conducted in this way: H_2O_2 was divided into 2 portions (0.2 mL) and added at the beginning and after 2 h. The mixture was thoroughly stirred with an overhead mechanical stirrer at 60 °C, and samples for analysis were taken at 1 h intervals. After the reaction, the catalyst was washed with isooctane and used in further catalytic experiments.

The synthesis of **ZIL** 4-(3′-ethylimidazolium)-butanesulfonate as to reaction given below was described in [24].

Table 1
Compositions of the electrolytes and designations of the catalysts.

Electrolyte			Designation of the catalysts
Base electrolyte (**BE**), mol/L	Additive (precursor), mol/L	pH	
0.1 Na_2WO_4 + 0.1 CH_3COOH (**BE1**)	–	6.8	Ti/W
BE 1	0.04 $Mn(CH_3COO)_2$	6.8	Ti/W,Mn
BE 1	0.04 $Zn(CH_3COO)_2$	6.8	Ti/W,Zn
0.1 Na_2WO_4 + 0.84 CH_3COOH + 0.01 NaOH (**BE2**)	–	5.5	Ti/W-2

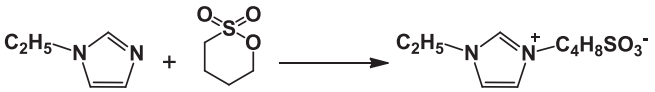

To obtain a catalyst with ZIL coating, the piece of PEO-coated sample was placed in an aqueous solution of 4-(3′-ethylimidazolium)-butanesulfonate in a mass ratio 1:1 (PEO-coated sample:ZIL) and stirred for 2 h at room-temperature. Then the sample with ZIL was dried at 80 °C and used in the catalysis and phys-chemical studies.

Quantitative analysis of the organic phase of the reaction mixture was carried out by gas liquid chromatography on a Kristall 4000 instrument equipped with a Zebron ZB-1 capillary column of a length of 30 m (100% dimethylpolysiloxane as the liquid phase) and a flame ionization detector. The contents of substrates and oxidation products were determined with linear temperature programming in the 90–220°C range by the internal reference method.

The desulfurization of diesel fuel (S 1080 ppm) was described in [24]. The fuel (10 mL) and the catalyst (0.02 g) were placed into a thermostated reactor and heated up to 60 °C; then H_2O_2 (0.4 mL) was added. In some experiments, samples with ZIL coating (0.04 g) were used. After 4 h, the mixture was washed by DMF and refined fuel is analyzed by X-ray fluorescence spectrometry using ASE-2 sulfur analyzer. With fractional loading, the oxidant was added by 2 portions (0.2 mL); wherein the second portion of H_2O_2 (0.2 mL) was added to the refined by DMF fuel with used catalyst, the stirring was carried out for another 4 h.

3. Results and discussion

3.1. PEO coating compositions (features of plasma electrolytic formation and coating composition)

Table 1 indicates electrolyte compositions and catalyst designations. Tungstate base electrolytes (BE1 and BE2) are colorless solutions. When pink manganese acetate solution was added to them, a colloidal precipitate apparently consisting of manganese (II) tungstate and/or hydroxide was formed. During the PEO process, the disperse system acquired a brown color, probably because of the oxidation of manganese (II) with the formation of dispersed particles of MnO_2. Agitating the electrolyte kept them in suspension.

When zinc acetate was added to the acidified tungstate solution, a small amount of a white colloidal precipitate was initially formed, which was probably zinc (II) hydroxide. In addition, under these conditions, zinc paratungstate and sodium tungstozincates, which are readily soluble in water, could be formed [33,34]. During the PEO process, the white precipitate disappeared, and the electrolyte acquired a bright blue color. The formation of tungsten blue indicated a partial reduction of tungsten to an average valence of $5 < n < 6$. Since the anodic and cathodic spaces were not separated in the electrochemical cell for PEO, the hydrogen (at the moment of release) and zinc formed at the cathode could act as reducing agents: $H^+ + e^- \rightarrow H^0$; $Zn^{2+} + 2e^- \rightarrow Zn^0$. In addition, hydrogen was also formed on the anode as a result of thermolysis of water in the areas exposed to spark and/or microarc electric discharges during PEO [35].

Table 2 shows data on the elemental and phase composition of the coatings. The content of W in all coatings is approximately the same — 15.8–18.7 at. %. The oxygen concentration varies from 65.6 to 74.0 at. %. When manganese or zinc acetates are introduced into the electrolytes, these metals are found in the coating composition (5.3 at.% Zn and 7.3 at.% Mn). The detected carbon may be due to contamination of the coatings during handling, as well as the presence of acetate ions in electrolytes. The reasons for the presence of carbon in PEO coatings were discussed in detail in Refs. [36, 37].

The elemental and phase compositions of the coatings (Table 2) are in good agreement with the formulas and states of the electrolytes. In base electrolytes without the addition of manganese and zinc acetates, PEO coatings with WO_3 and TiO_2 are formed. When manganese acetate is added to the base electrolyte, the formed coatings contain TiO_2, WO_3, and $MnWO_4$. The presence of manganese tungstate in the coatings is apparently associated with the incorporation of Mn-containing dispersed particles from a colloidal electrolyte and their subsequent high temperature transformations in the channels of electrical breakdowns. When zinc acetate is introduced into the base electrolyte, tungsten blue is formed during PEO, and $Zn_{0.3}WO_3$ zinc-tungsten bronze may be present in the coatings, according to weak reflections on XRD patterns. Note that air annealing such samples at 700 °C leads to crystallization of $ZnWO_4$ in them; therefore, one can assume that amorphous or fine crystalline zinc tungstate is present in the initial coatings too. All the coatings formed have salad-green color due to the high content of tungsten trioxide in the surface layer.

Fig. 1 shows examples of SEM images of the surface of PEO coatings. The surface morphology of coatings formed in tungstate electrolytes (Fig. 1a, b) is typical for PEO layers: pores are randomly distributed on the surface, the sizes and density (number of pores per surface unit) of which depend on the pH of the electrolyte. The thickness of the coatings is 9–16 μm (Table 2). The addition of zinc acetate to the tungstate electrolyte leads to an increase in size and a decrease in density of the pores (Fig. 1c) with an increase in coating thickness to 27 μm. The addition of manganese acetate to the tungstate electrolyte reduces the thickness to 4 μm and sharply changes the surface morphology of the formed oxide layers: large pores disappear and the surface becomes more developed (Fig. 1d), apparently due to the incorporation of dispersed particles from the colloidal electrolyte.

3.2. Catalytic tests

Fig. 2 shows typical time dependences of thiophene conversion at single and fractional H_2O_2 loading for titanium-supported catalysts including those containing WO_3 without manganese or zinc (Fig. 2a) and those containing WO_3 and $MnWO_4$ or $ZnWO_4$ (Fig. 2b). Note that in all cases, fractional loading of peroxide contributes to an increase in the conversion of thiophene.

Analysis of Fig. 2a shows that Ti/W samples are more active than Ti/W-2 (Fig. 2a); therefore, tungstate electrolyte with a pH 6.8 is preferable for coating formation than electrolyte with a pH 5.5. That is why we further used BE1 electrolyte with the addition of acetates of the corresponding metals for obtaining W-, Mn-containing and W-, Zn-containing PEO coatings (Table 1).

Table 2
The average elemental compositions of PEO coatings formed in various base electrolytes with the addition of 0.04 mol/L $Mn(CH_3COO)_2$ or $Zn(CH_3COO)_2$.

Catalyst	Thickness of coating, μm	Phase composition of PEO coating	Elemental composition, at. %					
			C	O	Ti	W	Mn (Zn)	Na
Ti/W	9 ± 1	Ti + WO_3	–	71.1	10.3	18.7	–	–
Ti/W,Mn	4 ± 1	TiO_2 (a), WO_3, $MnWO_4$	–	65.6	10.3	16.8	7.3	–
Ti/W,Zn	27 ± 1	WO_3, ?$Zn_{0.3}WO_3$	5.0	65.6	6.4	17.7	5.3	–
Ti/W-2	16 ± 1	TiO_2 (a), WO_3, ?$Na_{0.28}WO_3$	–	74.0	9.3	15.8	–	0.9

Note: (?) - the presence of this phase is possible; TiO_2 (a) - anatase.

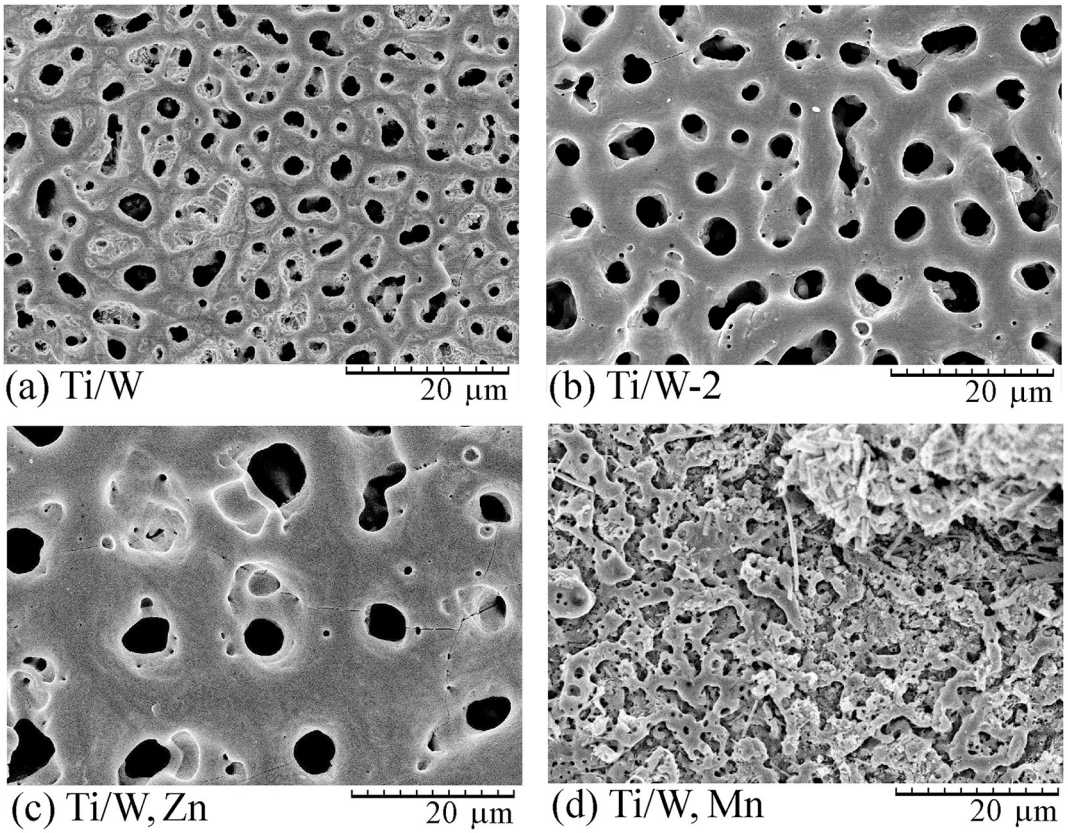

Fig. 1. SEM images of the surface of PEO-coated samples containing: (a, b) W, (c) W and Zn, (d) W and Mn. Signatures correspond to the notation in Table 1.

Of the studied samples, Ti/W, Zn showed the highest activity (Fig. 2b, c). The higher activity of W-, Zn-containing samples correlates with the presence of zinc-tungsten bronze in their composition (Table 2). At the same time, microscopic studies with high resolution reveal crystal-like formations with approximately equal concentrations of tungsten and zinc on the surface of the coatings (Fig. 3), which indicates the presence of amorphous zinc tungstate in their composition. It is known that amorphous compounds often have higher reactivity than crystalline ones. It is possible that both bronze and zinc tungstate determine a higher activity of Ti/W, Zn samples.

Table 3 presents the results of the catalysts test in five consecutive reaction cycles with a single loading of H_2O_2. It can be seen that all the catalysts gradually lose their weight and activity, but to a lesser extent, a loss of activity is observed for the W-, Zn-containing sample. The rather low activity of Ti/W, Mn samples in comparison with Ti/W samples can be associated with their smaller thickness.

Since the best results (the highest activity and its smallest decrease) were obtained using Ti/W, Zn catalyst, catalytic tests in the desulfurization of various S-containing organic compounds were carried out specifically for it (Fig. 4). In addition, the effect of additional deposition of ZIL on catalytic activity of Ti/W, Zn was clarified upon a single and fractional loading of H_2O_2. These data, as well as the results of desulfurization of real diesel fuel are summarized in Table 4.

Analysis of Fig. 4 and Table 4 shows that the ways proposed of fractional loading of the oxidizing agent and treatment of the catalyst by ZIL are very effective for increasing the conversion of organosulfur substrates and producing diesel fuel that meets modern environmental requirements (sulfur content < 10 ppm).

As can be seen from Fig. 4, the catalytic activity of the Ti/W, Zn decreases by the fifth cycle (conversion is reduced by 20–25%), but after ZIL treatment it does not change from cycle to cycle.

3.3. Behavior of Ti/W, Zn with and without ZIL

3.3.1. Appearance of samples before and after catalysis

The structure of the Ti/W, Zn catalyst has been investigated at different stages of its preparation and use in catalysis. Photographs of samples before (Ti/W, Zn) and after applying ZIL (Ti/W, Zn + ZIL), as well as after 5 cycles of catalytic oxidation of thiophene (Ti/W, Zn (Cat) and Ti/W, Zn + ZIL (Cat)) are shown in Fig. 5. The surface of the initial sample Ti/W, Zn is homogeneous and has green color. When the sample was cut, the outer layer of green color (I) partially peeled off, leaving the inner layer of gray color (II), Fig. 5a. After applying ZIL, white spherical translucent drops of ZIL appeared on the surface of both the initial coating I and the underlying layer II, Fig. 5b. These spherical regions are presented both in the form of individual droplets ~40–50 μm in size and in the form of their clusters.

After 5 cycles of thiophene oxidation, green areas were not found on PEO-coated samples with (Fig. 5d) and without ZIL (Fig. 5c). Rounded darker areas with dimensions of ~100–350 μm are visible on the surface. These may be traces of etching or corrosion. There are translucent light drops of ZIL on the surface of Ti/W, Zn + ZIL and Ti/W, Zn + ZIL (Cat) samples. In the second case, the drops are visible on the right edge of the sample in Fig. 5d. This indicates that after 5 cycles of thiophene oxidation, ZIL still remains on the surface of the samples.

From the analysis of Fig. 5, it follows that in the first cycle of catalysis, we investigated the samples, on the surface of which there were both outer green layer and inner gray layer (Fig. 5a). After five test cycles, no green layers were detected (Fig. 5c). Given the weight loss of Ti/W, Zn sample in 5 cycles of thiophene oxidation (Table 3), one can assume that the loss of catalytic activity is associated with a decrease in the thickness of the PEO layer. To understand the reasons for the operation of the catalyst, it is necessary to establish the evolution of the morphology and composition of the coating.

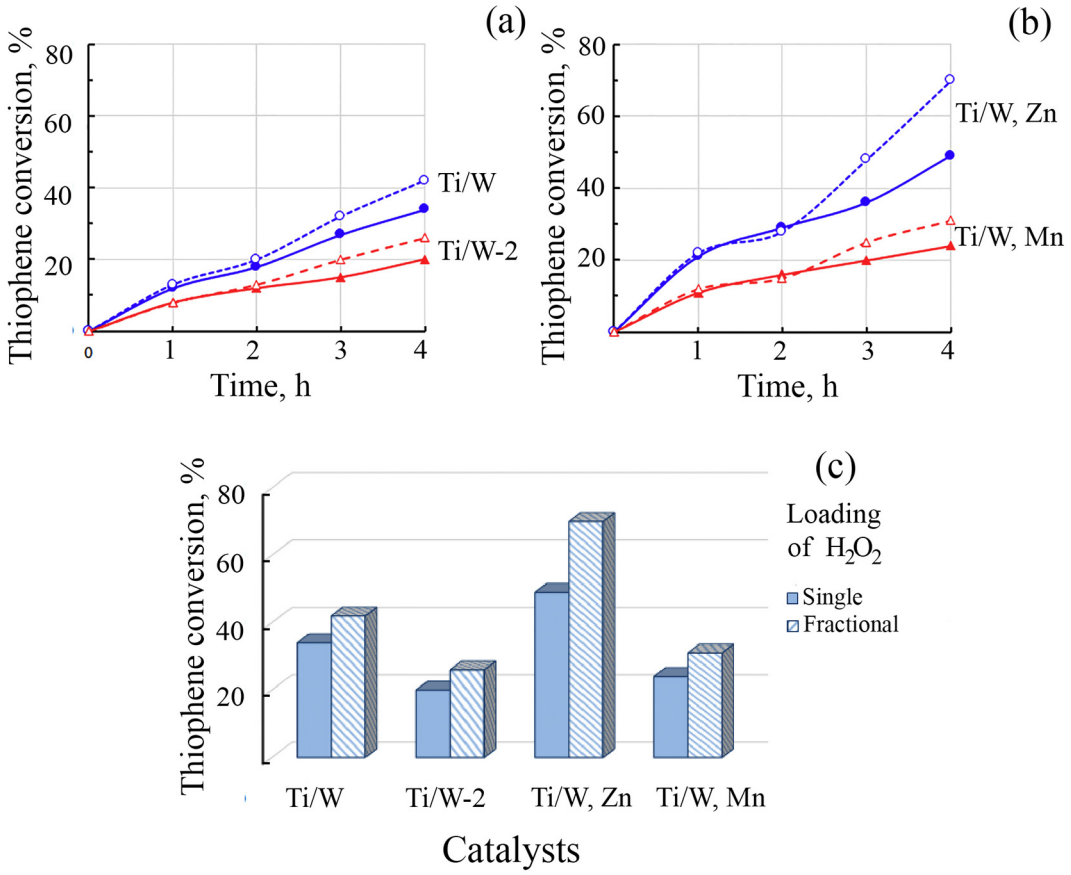

Fig. 2. Time dependences of thiophene conversion, comparison of single (straight line) and fractional loadings (dashed line) for the samples: (a) Ti/W and Ti/W-2, (b) Ti/W, Zn and Ti/W, Mn; and (c) thiophene conversion in 4 h with a single (2) and fractional (2) loading of H_2O_2. Reaction conditions: 60 °C, 0.1 g of catalyst, 0.4 mL of 50% H_2O_2, 4 h.

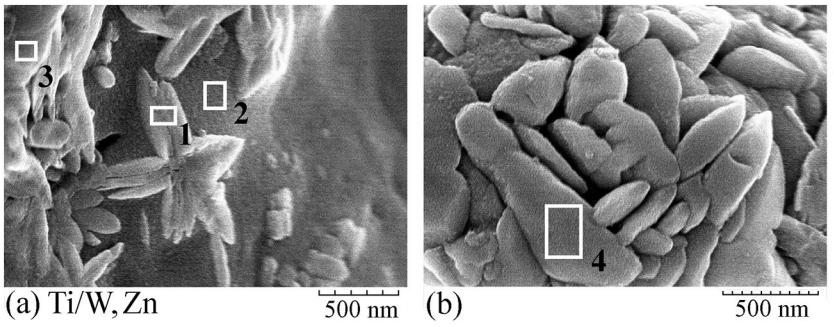

Elemental composition

Element	C, at. %			
	1	2	3	4
C	15.7	19.7	16.4	12.9
O	56.5	49.7	61.8	59.0
Ti	2.4	2.9	-	-
Zn	11.1	8.2	10.3	15.7
W	14.3	19.6	11.6	12.4

Fig. 3. Morphology and composition of individual surface areas of W-, Zn-containing PEO coating.

Table 3
Conversion (%) of thiophene in five consecutive oxidation cycles on different catalysts.

The sample	Cycle number					Loss of activity in 5 cycles, %	Weight loss in 5 cycles, %
	1	2	3	4	5		
Ti/W	34	31	31	29	26	24	2.4
Ti/W-2	20	21	19	17	15	25	2.9
Ti/W,Mn	24	23	23	20	18	25	4.3
Ti/W,Zn	49	50	48	45	39	20	4.8

Reaction conditions: T = 60 °C, m = 0.1 g of catalyst, single loading of 0.4 mL of 50% H_2O_2.

3.3.2. SEM studies of samples before and after catalysis

Fig. 6a shows the surface morphology of the coatings in the cleavage region (peeling of green layer). According to our estimates, based on this image, the thickness of the cleavage (or green layer) is ~4–7 μm, while the total thickness of PEO coatings is ~27 μm (Table 2). Comparing the element distribution maps (Fig. 6c) and the PEO coating morphology in the cleaved area (Fig. 6a) shows that Zn, W, O, Ti are present in I and II areas. Different signal intensities from both areas on the element distribution maps can be associated with different surface levels with respect analyzer.

The elemental compositions of I and II areas were determined by scanning at least 5 sites with subsequent averaging of data. An example of the selected sites, whose elemental composition was determined, is shown in Fig. 6a. The elemental compositions of I and II areas (Fig. 6) are close to the average that of the initial Ti/W, Zn sample (Table 5).

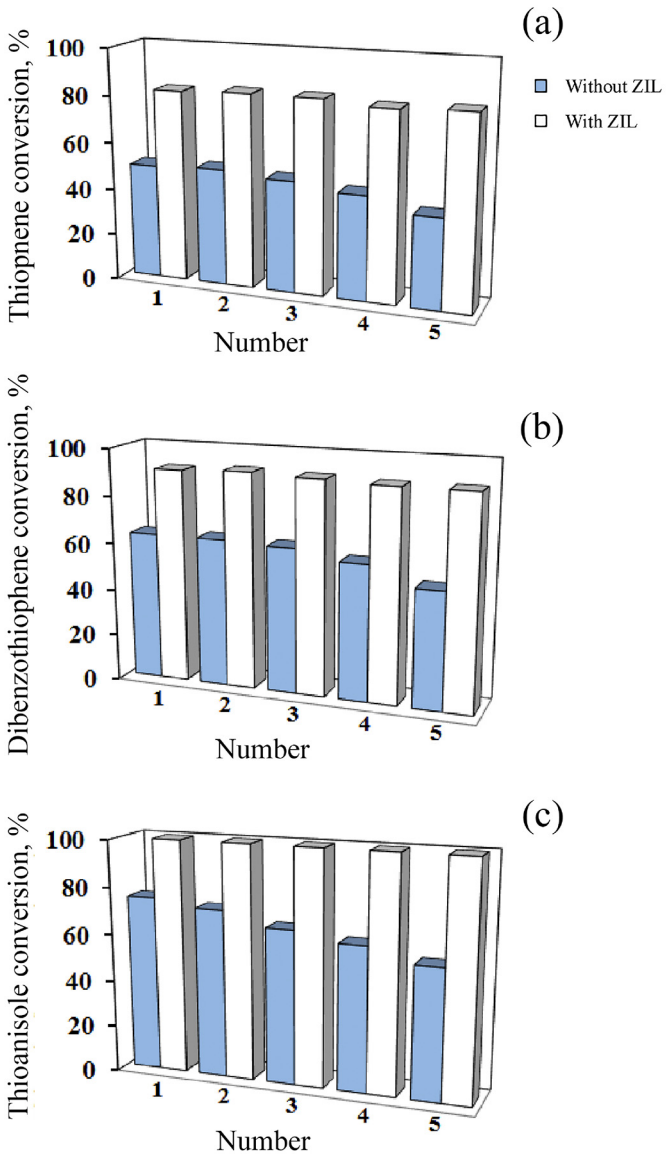

Fig. 4. Conversion of thiophene (a), dibenzothiophene (b) and thioanisole (c) on Ti/W, Zn and Ti/W, Zn + ZIL samples in 5 cycles of catalytic tests with a single loading of H_2O_2 as oxidizer. Reaction conditions: 60 °C, 0.1 g of catalyst Ti/W, Zn or Ti/W, Zn + ZIL, a single loading of 0.4 mL of 50% H_2O_2, 4 h for (a, b) and 0.25 h for (c). Blue – without ZIL, white – with ZIL.

Table 4
Conversion (%) of thiophene, thioanisole, dibenzothiophene and oxidative desulphurization of diesel fuel on Ti/W, Zn catalyst with and without ZIL.

Substrate	Process time, h	Conversion, % (residual sulfur content, ppm)		
		Ti/W,Zn	Ti/W,Zn + ZIL	Ti/W,Zn + ZIL
		Single loading (0.4 mL H_2O_2)		Fractional loading (0.2 + 0.2 mL H_2O_2)
Thiophene	4	49	82	93
Thioanisole	0.25	75	100	100
Dibenzothiophene	4	63	91	98
Diesel fuel	4	94 (65)	97 (35)	99.6 (6)

Reaction conditions: T = 60 °C, 50% H_2O_2.

Smooth (1) and rough (2) areas are observed on the surface of the II inner layer (Fig. 6b). Their average compositions are close to each other and practically do not differ from the composition of I and II areas. Consequently, the elemental composition of the surface in the cleavage region differs slightly in the transition from the outer green layer to the inner gray layer. Obviously, the initial coating consists of at least two layers. Above the dense dark gray layer adjacent to the metal, there is a green layer penetrated by large pores. Since both layers are similar in terms of the content of the main elements, including the tungsten content, the difference in their color is due to a change in the oxidation state of tungsten. WO_3 gives the green color to the outer layer, and the gray color of the inner layer obviously indicates the presence of W in the oxidation state $5 < n < 6$, for example, in the form of non-stoichiometric tungsten oxide WO_{3-x} or tungsten bronzes.

The surface of Ti/W, Zn (Cat) sample after 5 cycles of catalytic testing is shown in Fig. 7a. The morphology of the coating surface after 5 cycles of catalytic tests is close to that of the cleaved surface (area II in Fig. 6). At higher resolution (Fig. 7b), it is seen that the surface is rough with uplifts and depressions. The etched coral-like structure indicates the processes of selective leaching of individual areas of the coating. Among the features of the surface structure, one can note the presence of exposed sites of titanium substrate (area 4 in Fig. 7c contains 99.7 at. % Ti). Their presence is consistent with dark spots on the sample surfaces in Fig. 5c. From the analysis of Fig. 7c it follows that the thickness of the stored oxide layer on titanium is ~ 1 μm, i.e., after 5 cycles of catalytic tests, the layer thickness decreased from ~20 to ~1 μm. Elemental composition of the stored oxide layer noticeably differs from the composition of surface layer before catalytic tests, Table 5 and Fig. 7. The tungsten concentration decreased by ~9 times, the zinc content became very low, and the titanium concentration increased by 5 times. All these facts indicate that the catalytic layer is being washed off from cycle to cycle. As was shown earlier [23,24,38], such leaching can be a consequence of the action of sulfuric acid formed during the thiophene oxidation. Meanwhile, despite a decrease in the content of tungsten and zinc, the sample exhibits a rather high catalytic activity. For 5 cycles, the conversion of thiophene decreased by 20% (Table 3). This means that this catalyst is active in a wide range of tungsten and zinc concentrations in the TiO_2 oxide layer. Possibly, not only the oxide layer predominantly containing tungsten and zinc (as a sample in the first test cycle), but also W-, Zn-doped TiO_2 layer (the sample after 5 test cycles) possesses catalytic activity.

3.3.3. W-, Zn-containing PEO coating with ZIL

Fig. 8a shows the surface morphology of a Ti/W, Zn + ZIL sample in the cleaved region. The ZIL not only spreads over the surface of the entire sample, but also collects into spherical formations and their agglomerates (Fig. 8). Note that in the case of surface I, globular clusters of ZIL can fill individual pores (Fig. 8b).

Elemental composition data (Table 5) indicate that ZIL extends over the entire surface. Unlike the initial PEO coatings, the surface contains sulfur and a lot of carbon on - the consequences of applying ZIL. Low concentrations of the elements of the PEO coating (O, Ti, W and Zn) are associated with the presence of ZIL on the surface.

Fig. 9a shows a general view of the surface of the samples with ZIL after 5 cycles of catalytic tests. The surface morphology of the Ti/W, Zn + ZIL (Cat) sample is similar to the surface of the inner gray layer of the initial PEO coating (area II in Fig. 6a, b). Of the characteristic features, we note light spherical formations of different sizes. The concentration of titanium is lower and the concentration of tungsten and oxygen is higher in the lighter areas, than in the darker areas.

Compared to Ti/W, Zn(Cat) samples, the surface of Ti/W, Zn + ZIL (Cat) samples has a significantly higher tungsten content and lower titanium content (Table 5). This means that the application of ZIL significantly reduces the rate of leaching of the coating components, i.e., it stabilizes the oxide layer under experimental conditions. The uniform distribution of sulfur, which is part of the ZIL (Fig. 9b), indicates

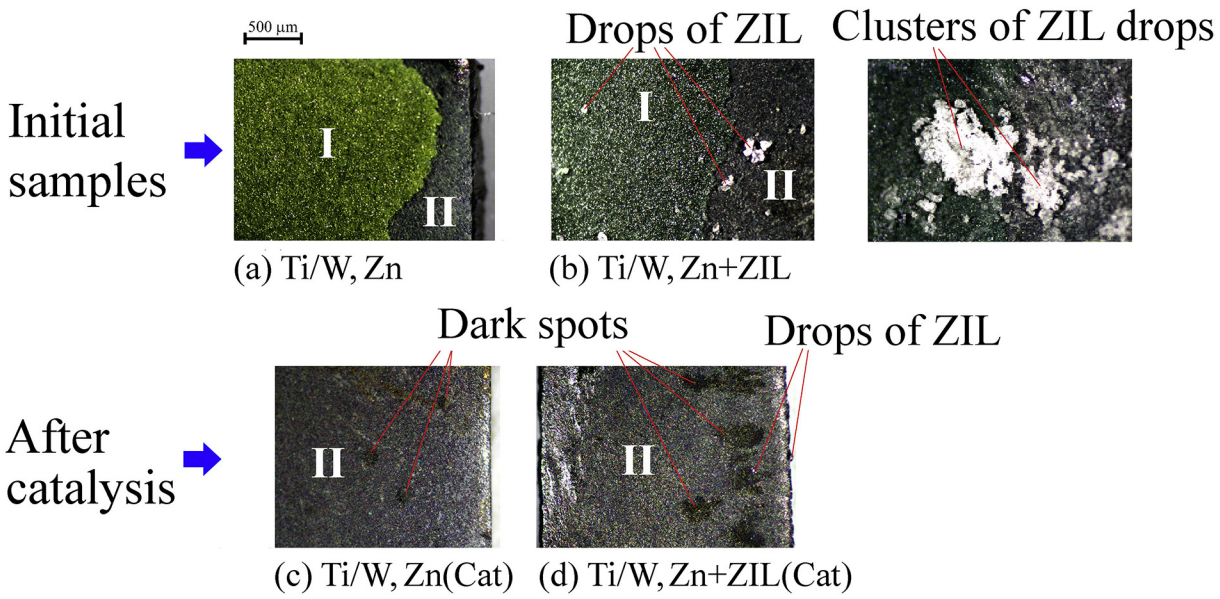

Fig. 5. Appearance of samples: (a) Ti/W, Zn - initial sample; (b) Ti/W, Zn + ZIL - the sample with zwitterionic liquid, (c) Ti/W, Zn(Cat) - the initial sample after 5 cycles of catalytic tests in peroxide oxidation of thiophene; (d) Ti/W, Zn + ZIL(Cat) - the sample with zwitterionic liquid after 5 cycles of catalytic tests in thiophene peroxide desulfurization.

uniform wetting of the surface by ZIL. An increase in the conversion of organosulfur compounds after the application of ZIL (Fig. 4) indirectly indicates that catalysis processes are mainly associated with the surface of the sample, and not with dispersed coating particles that have passed into solution. On the other hand, it is possible that the ZIL itself, deposited on the oxide layer, has catalytic properties. However, as to [23], when using only 4-(3′-ethylimidazolium)-butanesulfonate, the conversion of thiophene in the model reaction is about 15%.

Table 5
The effect of zwitterionic liquid and catalytic tests on the average elemental composition of the outer catalyst layer of Ti/W, Zn catalyst.

Catalyst	Elemental composition, at. %					
	C	O	S	Ti	W	Zn
Ti/W,Zn	5.0	65.6	–	6.4	17.7	5.3
Ti/W,Zn + ZIL	46.6	38.3	3.3	3.5	6.3	2.0
Ti/W,Zn(Cat)	17.7	47.3	–	33.0	1.9	0.1
Ti/W,Zn + ZIL(Cat)	32.1	44.1	0.4	16.0	7.2	0.1

4. Discussion

As follows from the data obtained, W-, Zn-containing PEO coatings have a layered structure — the outer green layer is enriched with zinc and WO_3, the inner layer adjacent to the substrate is enriched with titanium, and the intermediate gray layer has a composition similar to that of the green layer.

During catalysis, the studied W-containing PEO coatings are gradually leached from cycle to cycle, but continue to act as catalysts of desulfurization. From the fact that the catalytically active layers are leached, it follows that they have their own resource, and the catalysts have their own service life. It should be noted that after the end of this resource, the catalytically active layers could be easily regenerated as a result of repeated PEO treatment in the same electrolyte, which is an advantage of this method. In addition, the results of the studies show that the use of ZIL and fractional loading of the oxidizing agent not only increases their activity, but also reduces the loss of the active layer. As was shown in [24], the deposition of ZIL on Ce-, Zr-containing PEO coating also increased their activity and stability. It can be assumed that the use of ZIL will increase the activity and stability of any coating that has at least the slightest catalytic activity.

Even after leaching, W-, Zn-containing PEO coatings continue to catalyze the reaction of oxidative desulfurization. This means that all three layers — the outer layer enriched with W and Zn, the intermediate layer, apparently containing non-stoichiometric tungsten

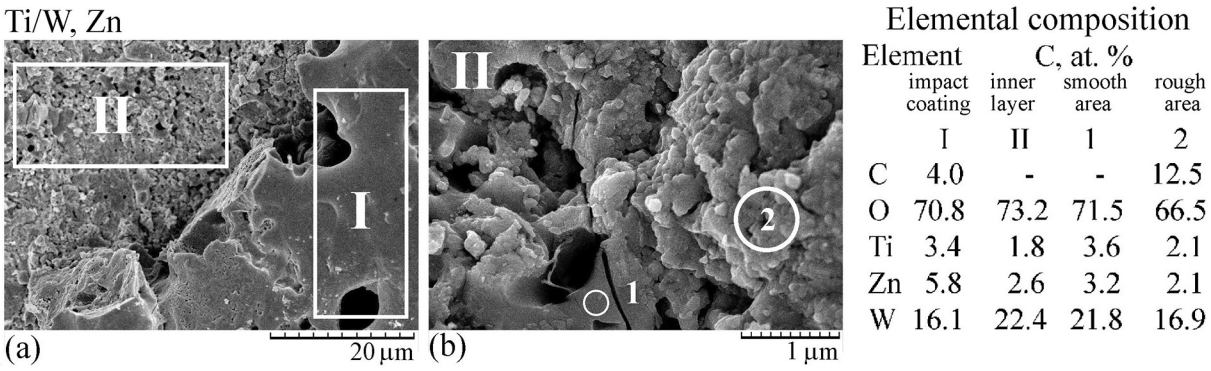

Fig. 6. Initial Ti/Zn, W sample in the area of peeling: (a, b) SEM images of intact PEO coating (I) and inner layer (II) after peeling, (b) smooth (1) and rough (2) areas of inner layer II, and averaged elemental composition of corresponding areas.

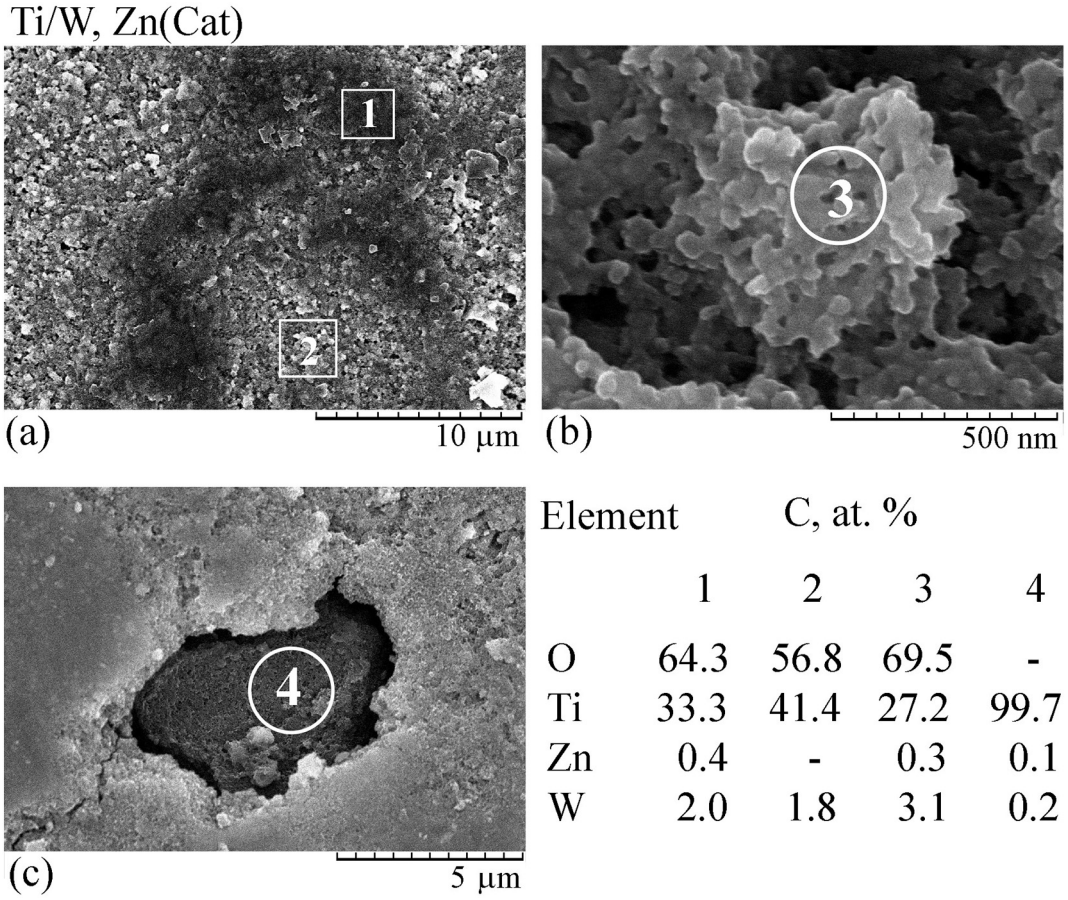

Element	C, at. %			
	1	2	3	4
O	64.3	56.8	69.5	-
Ti	33.3	41.4	27.2	99.7
Zn	0.4	-	0.3	0.1
W	2.0	1.8	3.1	0.2

Fig. 7. SEM images of the surface of Ti/W, Zn(Cat) sample after 5 cycles of catalytic tests in peroxide oxidation of thiophene and elemental concentrations in the areas: 1 – dark site, 2 – light site, 3 – coral-like site, 4 – pore bottom.

oxides or tungsten bronzes, and the inner layer, which is titanium dioxide doped with tungsten and zinc, possess catalytic activity in thiophene oxidation. Therefore, the coatings are catalytically active in a wide range of tungsten and zinc concentrations (from the first to the fifth cycle). From the data obtained it follows that it is not necessary to introduce so much tungsten and zinc into the coatings. Perhaps, it is enough to dope a layer of TiO_2 or other more corrosion-resistant complex oxide systems with tungsten and zinc.

5. Conclusions

W-containing oxide layers including those enriched with Mn or Zn were formed on titanium by the plasma electrolytic oxidation in acidified sodium tungstate solution additionally containing acetate of manganese (II) or zinc (II). Oxide layers containing, along with titanium and oxygen, 15.8–18.7 at. % W, up to 5.3 at.% Zn or 7.3 at.% Mn were obtained. All oxide systems exhibit some catalytic activity in the thiophene oxidation with hydrogen peroxide. Their activities are reduced

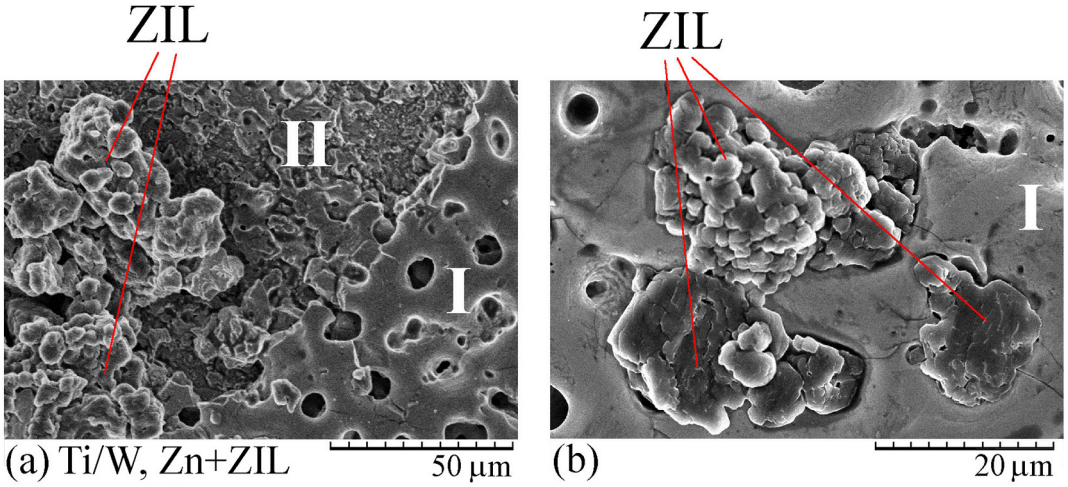

Fig. 8. SEM images of the surface of Ti/W, Zn + ZIL sample: (a) ZIL drops on the surface of inner layer of PEO coating after peeling II, (b) ZIL drops in the pores of impact PEO coating I.

(a) Ti/W, Zn+ZIL(Cat)

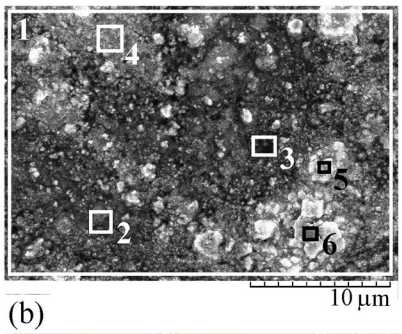

Elemental composition

Element	C, at. %					
	Surf.	Dark sites			Light sites	
	1	2	3	4	5	6
O	73.5	-	-	72.5	83.6	90.8
Ti	18.6	93.7	79.8	25.2	5.3	-
Zn	0.5	-	0.3	0.2	0.5	0.04
W	7.5	6.3	19.9	2.1	10.6	9.15

(b)

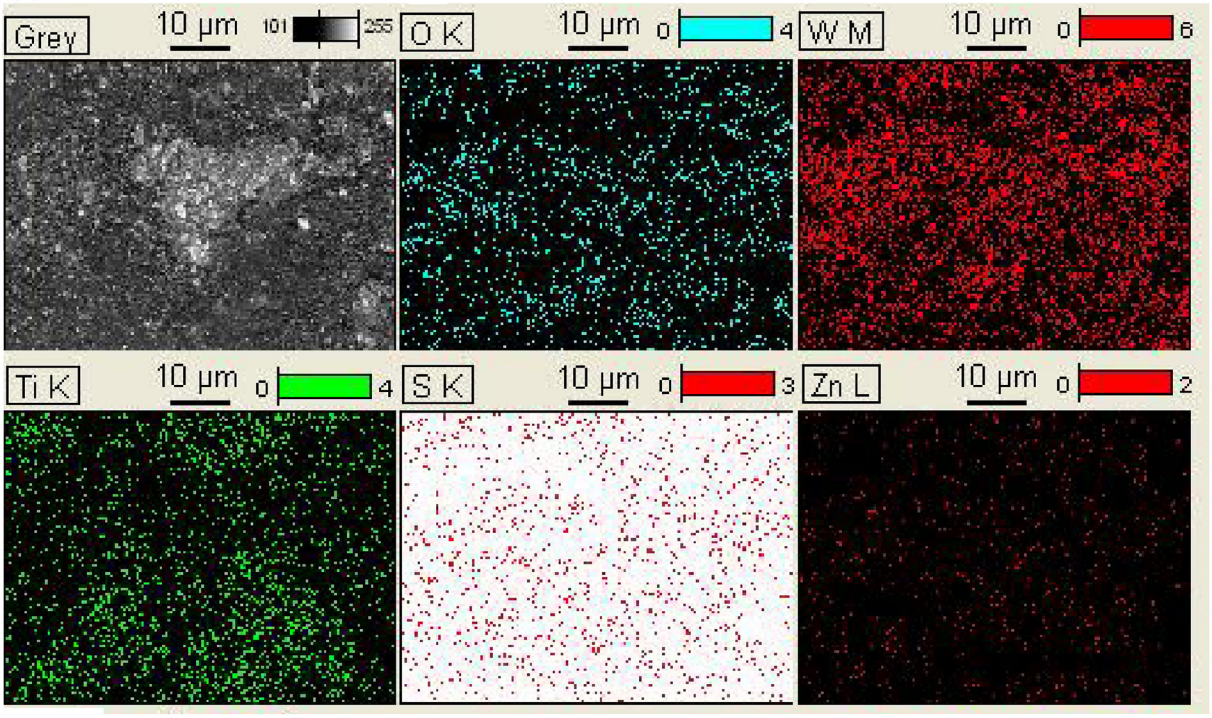

Fig. 9. SEM images of the surface of Ti/W, Zn + ZIL(Cat) sample after 5 cycles of catalytic tests in peroxide oxidation of thiophene and elemental compositions of dark and light sites 1–6 (a); element distribution maps (b).

by 20–25% after 5 cycles of catalytic tests.

The maximum catalytic activity of W-, Zn-containing PEO coatings among the samples under study can be related with their largest thickness and with the possible presence of crystalline $Zn_{0.3}WO_3$ and amorphous $ZnWO_4$ in their composition. Scanning electron microscopy together with energy dispersive analysis have showed that W-, Zn-containing PEO coatings have a layered structure with W-, Zn-enriched outer green layer, intermediate gray layer of similar composition and W-doped titania inner layer. A decrease in the activity of such catalysts may be due to surface etching as a result of producing sulfuric acid during this reaction.

It has been established that applying a zwitterionic liquid, such as 4-(3′-ethylimidazolium)-butanesulfonate, to the surface of Ti/W, Zn catalyst increases its activity in oxidative desulfurization of thiophene, dibenzothiophene and thioanisole by 30–40% with a single loading of hydrogen peroxide. The conversion of these S-containing compounds was not changed during five consecutive cycles of catalytic tests. According to SEM, zwitterionic liquid forms a thin film and fills the pores on the surface, thereby protecting the catalyst from etching. With fractional loading of hydrogen peroxide, the proposed W-, Zn-containing catalyst with zwitterionic liquid has allowed removing sulfur from diesel fuel to the residual content 6 ppm that meets the modern environmental requirements.

CRediT authorship contribution statement

A.A. Bryzhin: Validation, Investigation.**I.G. Tarkhanova:**Writing - original draft, Writing - review & editing, Funding acquisition.**M.G. Gantman:**Methodology, Investigation, Formal analysis.**V.S. Rudnev:**Conceptualization, Project administration, Funding acquisition.**M.S. Vasilyeva:**Methodology, Investigation, Resources, Writing - review & editing.**I.V. Lukiyanchuk:**Writing - original draft, Writing - review & editing.

Declaration of competing interest

The authors declare that they have no known competing financial interests or personal relationships that could have appeared to influence the work reported in this paper.

Acknowledgements

The work was carried out within the Institute of Chemistry FEB RAS State Order (project no. 265-2018-0001) and funded by the Russian Foundation for Basic Research (project no. 19-33-90024).

References

[1] M. Mohedano, X. Lu, E. Matykina, C. Blawert, R. Arrabal, M.L. Zheludkevich, Plasma electrolytic oxidation (PEO) of metals and alloys, in: Klaus Wandelt (Ed.), Encyclopedia of Interfacial Chemistry, Surface Science and Electrochemistry, Corrosion and Passivation, 6.1 Elsevier Inc., New York, 2018, pp. 423–438, , https://doi.org/10.1016/B978-0-12-409547-2.13398-0.

[2] T.W. Clyne, S.C. Troughton, A review of recent work on discharge characteristics during plasma electrolytic oxidation of various metals, Int. Mater. Rev. 64 (3) (2019) 127–162, https://doi.org/10.1080/09506608.2018.1466492.

[3] X.Y. Liu, K. Wang, Y. Zhou, X.Y. Tang, X.H. Zhu, R.S. Zhang, X.L. Zhang, X. Jiang, B.D. Liu, In-situ fabrication of noble metal modified (Ce, Zr)O_2-delta monolithic catalysts for CO oxidation, Appl. Surf. Sci. 483 (2019) 721–729, https://doi.org/10.1016/j.apsusc.2019.03.315.

[4] S.F. Tikhov, G.V. Chernykh, V.A. Sadykov, A.N. Salanov, G.M. Alikina, S.V. Tsybulya, V.F. Lysov, Honeycomb catalysts for clean-up of diesel exhausts based upon the anodic-spark oxidized aluminium foil, Catal. Today 53 (4) (1999) 639–646, https://doi.org/10.1016/S0920-5861(99)00160-1.

[5] M.V. Ved, N.D. Sakhnenko, A.V. Karakurkchi, T.Y. Myrna, Functional mixed cobalt and aluminum oxide coatings for environmental safety, Funct. Mater. 24 (2) (2017) 303–310, https://doi.org/10.15407/fm24.02.303.

[6] K. Schierbaum, M. El Achhab, Generation of an electromotive force by hydrogen-to-water oxidation with Pt-coated oxidized titanium foils, Phys. Status Solidi A-Appl. Mat. 208 (12) (2011) 2796–2802, https://doi.org/10.1002/pssa.201127400.

[7] F. Patcas, W. Krysmann, Efficient catalysts with controlled porous structure obtained by anodic oxidation under spark-discharge, Appl. Catal. A-Gen. 316 (2) (2007) 240–249, https://doi.org/10.1016/j.apcata.2006.09.028.

[8] M.S. Vasilyeva, V.S. Rudnev, A.I. Tulush, P.M. Nedozorov, A.Y. Ustinov, WO_x, SiO_2, TiO_2/Ti composites, fabricated by means of plasma electrolytic oxidation, as catalysts of ethanol dehydration into ethylene, J. Phys. Chem. A 89 (6) (2015) 968–973, https://doi.org/10.1134/S0036024415060321.

[9] J. Xu, P. Holthaus, N.J. Yang, S.Y. Jiang, A. Heupel, H. Schonherr, B. Yang, X. Jiang, Catalytic tar removal using TiO_2/$NiWO_4$-Ni_5TiO_7 films, Appl. Catal. B-Environ. 249 (2019) 155–162, https://doi.org/10.1016/j.apcatb.2019.03.006.

[10] N. Salami, M.R. Bayati, F. Golestani-Fard, H.R. Zargar, UV and visible photodecomposition of organic pollutants over micro arc oxidized Ag-activated TiO_2 nanocrystalline layers, Mater. Res. Bull. 47 (4) (2012) 1080–1088, https://doi.org/10.1016/j.materresbull.2011.12.022.

[11] L. Yang, P. Zhang, Y. Liu, J. Liang, W.B. Tian, Y.M. Zhang, Z.M. Sun, Pretreatment on Ti substrate for Ti/Pt anode by electrolytic plasma processing, Trans. Inst. Metal Finish. 96 (4) (2018) 174–178, https://doi.org/10.1080/00202967.2018.1471035.

[12] M.N. Hossain, H.C. Park, H.S. Choi, A comprehensive review on catalytic oxidative desulfurization of liquid fuel oil, Catalysts 9 (3) (2019), https://doi.org/10.3390/catal9030229 Paper 229.

[13] M. Rezakazemi, Z. Zhang, Desulfurization materials, in: I. Dincer (Ed.), Comprehensive Energy Systems, 2 Elsevier Inc, 2018, pp. 944–979, , https://doi.org/10.1016/b978-0-12-809597-3.00263-7 Chapter 2.29.

[14] W. Abdul-Kadhim, M.A. Deraman, S.B. Abdullah, S.N. Tajuddin, M.M. Yusoff, Y.H. Taufiq-Yap, M.H.A. Rahim, Efficient and reusable iron-zinc oxide catalyst for oxidative desulfurization of model fuel, J. Environ. Chem. Eng. 5 (2) (2017) 1645–1656, https://doi.org/10.1016/j.jece.2017.03.001.

[15] X. Li, Y. Gu, H. Chu, G. Ye, W. Zhou, W. Xu, Y. Sun, MFM-300(V) as an active heterogeneous catalyst for deep desulfurization of fuel oil by aerobic oxidation, Appl. Catal. A Gen. 584 (2019) 117152, , https://doi.org/10.1016/j.apcata.2019.117152.

[16] H.L. Wang, R.J. Zhou, M.J. Jiang, Z.G. Lin, Y.Q. Deng, Ozonolysis mechanism of heterocyclic organic sulfides: a computational study, Comput. Theor. Chem. 1090 (2016) 88–93, https://doi.org/10.1016/j.comptc.2016.06.015.

[17] X.D. Tang, L.L. Shui, L. Liu, Catalytic oxidative desulfurization of straight-run diesel by using NO_x and air as oxidants, Chin. J. Catal. 25 (10) (2004) 789–792 (WOS:000225246600006).

[18] M.A. Safa, R. Bouresli, R. Al-Majren, T. Al-Shamary, X. Ma, Oxidative desulfurization kinetics of refractory sulfur compounds in hydrotreated middle distillates, Fuel 239 (2019) 24–31, https://doi.org/10.1016/j.fuel.2018.10.141.

[19] R. Ghubayra, C. Nuttall, S. Hodgkiss, M. Craven, E.F. Kozhevnikova, I.V. Kozhevnikov, Oxidative desulfurization of model diesel fuel catalyzed by carbon-supported heteropoly acids, Appl. Catal. B Environ. 253 (2019) 309–316, https://doi.org/10.1016/j.apcatb.2019.04.063.

[20] M.I.S. de Mello, E.V. Sobrinho, V.L.S.T. da Silva, S.B.C. Pergher, V or Mn zeolite catalysts for the oxidative desulfurization of diesel fractions using dibenzothiophene as a probe molecule: preliminary study, Mol. Catal. 482 (2020) 100495, , https://doi.org/10.1016/j.mcat.2018.02.009.

[21] I.S. Tomskii, M.V. Vishnetskaya, P.A. Vakhrushin, L.A. Tomskaya, Oxidative desulfurization of straight-run diesel fraction on vanadium-molybdenum catalysts, Petrol. Chem. 57 (10) (2017) 908–913, https://doi.org/10.1134/S0965544117100188.

[22] B. Mokhtari, A. Akbari, M. Omidkhah, Superior deep desulfurization of real diesel over MoO_3/silica gel as an efficient catalyst for oxidation of refractory compounds, Energy Fuel 33 (8) (2019) 7276–7286, https://doi.org/10.1021/acs.energyfuels.9b01646.

[23] V.S. Rudnev, I.V. Lukiyanchuk, M.S. Vasilyeva, V.P. Morozova, V.M. Zelikman, I.G. Tarkhanova, W-containing oxide layers obtained on aluminum and titanium by PEO as catalysts in thiophene oxidation, Appl. Surf. Science 422 (2017) 1007–1014, https://doi.org/10.1016/j.apsusc.2017.06.071.

[24] I.G. Tarkhanova, A.A. Bryzhin, M.G. Gantman, T.P. Yarovaya, I.V. Lukiyanchuk, P.M. Nedozorov, V.S. Rudnev, Ce-, Zr-containing oxide layers formed by plasma electrolytic oxidation on titanium as catalysts for oxidative desulfurization, Surf. Coat. Technol. 362 (2019) 132–140, https://doi.org/10.1016/j.surfcoat.2019.01.101.

[25] A.A.A. Bryzhin, V.S. Rudnev, I.V. Lukiyanchuk, M.S. Vasilyeva, I.G. Tarkhanova, The effect of the composition of oxide layers formed by plasma electrolytic oxidation on the mechanism of peroxide oxidative desulfurization, Kinet. Catal. 61 (2) (2020) 283–290, https://doi.org/10.1134/S0023158420020020.

[26] S.O. Ribeiro, D. Juliao, L. Cunha-Silva, V.F. Domingues, R. Valenca, J.C. Ribeiro, B. de Castro, S.S. Balula, Catalytic oxidative/extractive desulfurization of model and untreated diesel using hybrid based zinc-substituted polyoxometalates, Fuel 166 (2016) 268–275, https://doi.org/10.1016/j.fuel.2015.10.095.

[27] R. Fehrmann, A. Riisager, M. Haumann (Eds.), Supported Ionic Liquids: Fundamentals and Applications, Wiley-VCH, Weinheim, 2014, , https://doi.org/10.1002/9783527654789 (789 p).

[28] B.V. Romanovsky, I.G. Tarkhanova, Supported ionic liquids in catalysis, Russ. Chem. Rev. 86 (5) (2017) 444–458, https://doi.org/10.1070/RCR4666.

[29] Y.L. Bi, M.J. Zhou, H.Y. Hu, C.P. Wei, W.X. Li, K.J. Zhen, Oxidation of long chain primary alcohols to acids over the quaternary ammonium peroxotungstophosphate catalyst system, React. Kinet. Catal. Lett. 72 (1) (2001) 73–82, https://doi.org/10.1023/A:1010532514454.

[30] Z.P. Pai, D.I. Kochubey, P.V. Berdnikova, V.V. Kanazhevskiy, I.Y. Prikhod'ko, Y.A. Chesalov, Structure and properties of tungsten peroxopolyoxo complexes — promising catalysts for organics oxidation. I. Structure of peroxocomplexes studied during the stepwise synthesis of tetra(diperoxotungsten)phosphate-tetra-n-butyl ammonium, J. Mol. Catal. A-Chem 332 (1–2) (2010) 122–127, https://doi.org/10.1016/j.molcata.2010.09.007.

[31] A.A. Bryzhin, M.G. Gantman, A.K. Buryak, I.G. Tarkhanova, Bronsted acidic SILP-based catalysts with $H_3PMo_{12}O_{40}$ or $H_3PW_{12}O_{40}$ in the oxidative desulfurization of fuels, Appl. Catal. B-Environ. 257 (2019), https://doi.org/10.1016/j.apcatb.2019.117938 UNSP 117938.

[32] I.V. Lukiyanchuk, V.S. Rudnev, N.A. Andenko, T.A. Kaidalova, E.S. Panin, P.S. Gordienko, Anodic-spark oxidation of aluminum alloy in tungstate electrolytes, Russ. J. Appl. Chem. 75 (4) (2002) 573–578, https://doi.org/10.1023/A:1019560912922.

[33] G.M. Rozantsev, K.V. Yeroshyna, O.Yu. Mariichak, S.V. Radio, Synthesis of Zinc Paratungstate B, Series Chemical Sciences 1 Bulletin of Vasyl' Stus Donetsk National University, 2017, pp. 32–37 http://jvestnik-chemistry.donnu.edu.ua/article/view/4962/4996 (In Russian).

[34] Y.A. Moroz, Regularities of the synthesis of heteropolicompounds with 3d-elements, http://donnu.ru/public/journals/files/VestnikDonNU_A_2017_N1_compr.pdf (In Russian).

[35] L.O. Snizhko, The nature of anodic gas at plasma electrolytic oxidation, Prot. Met. Phys. Chem. Surf. 50 (6) (2014) 705–708, https://doi.org/10.1134/S2070205114060215.

[36] V.I. Vovna, S.V. Gnedenkov, P.S. Gordienko, M.V. Kuznetsov, S.L. Sinebryukhov, A.I. Cherednichenko, O.A. Khrisanfova, Surface layers produced on titanium by microarc oxidation: an X-ray diffractometry study, Russ. J. Electrochem. 34 (10) (1998) 1090–1093 (WOS:000076740800021).

[37] V.S. Rudnev, A.A. Vaganov-Vil'kins, A.Yu. Ustinov, P.M. Nedozorov, Carbon in oxide layers formed under electric discharge conditions, Prot. Met. Phys. Chem. Surf. 47 (3) (2011) 330–338, https://doi.org/10.1134/S2070205111030130.

[38] B.Y. Zhang, Z.X. Jiang, J. Li, Y.N. Zhang, F. Lin, Y. Liu, C. Li, Catalytic oxidation of thiophene and its derivatives via dual activation for ultra-deep desulfurization of fuels, J. Catal. 287 (2012) 5–12, https://doi.org/10.1016/j.jcat.2011.11.003.